Computational study of order-disorder transitions in alloy clusters using the isothermal-isobaric ensemble

Marie C. Vicéns and Gustavo E. López*
Department of Chemistry, University of Puerto Rico at Mayagüez, P.O. Box 9019, Mayagüez, Puerto Rico 00681-9019
(Received 22 December 1999; published 17 August 2000)

The low-temperature order-disorder transition for a Pd_7Ni_6 alloy cluster was considered using the isothermal-isobaric (*NPT*) ensemble. The ordered structure consists of a completely segregated arrangement of atoms and the disordered systems present a certain degree of mixing within the cluster. The transition was characterized by monitoring anomalies in the average value of the constant pressure heat capacity, $\langle C_p \rangle$, as a function of temperature. The maximum temperature in the $\langle C_p \rangle$ versus T graph, T_{mixing}, is used for estimating the equilibrium temperature at which the transition occurs, at a given pressure. It is observed that as the pressure increases, T_{mixing} decreases up to a value of 25 K, where the mixing transition becomes temperature-independent. The sampling difficulties presented in standard Monte Carlo simulations are circumvented by implementing the *J*-walking procedure to the *NPT* ensemble.

PACS number(s): 36.40.Ei, 65.40.+g, 05.10.Ln, 05.70.−a

I. INTRODUCTION

The properties of alloy clusters have been the subject of considerable research over the past few years. In particular, the structure, stability, and thermodynamics of clusters in vapor have been studied extensively. In the description of the structure of alloy clusters, three possible spatial arrangements of atoms have been proposed for systems of type *AB* [1,2]. The first one is called the cherry model and consists of a core rich in component *A* surrounded by a shell rich in component *B*. Another possible structure assumes that components *A* and *B* are randomly distributed over the cluster. The third possible structure is that *A* and *B* separate into two droplets of pure components. Figure 1 depicts these structures for a 13-atom alloy cluster. Various theoretical studies have explored the potential-energy surface (PES) of alloy clusters. In particular, our group has shown in previous studies [2,3] that for a Ni_7Pd_6 alloy cluster, the lowest energy equilibrium structure consists of two separate droplets of pure components. This structure, which is shown in Fig. 1(c), is known in this study as the completely segregated structure. The randomly distributed structure for this system is higher in energy and is called the mixed system.

Another active area of research involving finite systems, which is related to structural changes as a function of temperature, is the determination of cluster phase transitions. Various phase transitions have been identified [3–12] and associated with cluster isomerization in a certain temperature range. For example, the solid-liquid cluster equilibrium occurs in a temperature regime where solidlike and liquidlike forms of the cluster coexist [4–6,9,10]. In the case of alloy clusters in vapor, a low-temperature phase transition has been identified [3,11,12] that is associated with the order-disorder transition in bulk [13]. Specifically, at low temperatures a coexistence temperature regime exists where segregated and mixed forms of the cluster have been identified.

Most theoretical studies that consider phase transitions have been based on computer simulations in the canonical ensemble. However, a more thorough thermodynamic description can be obtained using the isothermal-isobaric ensemble. For example, Cheng *et al.* [9] used this ensemble to describe the solid-liquid transition for Ar_{55}. In that work, by identifying anomalies in the constant pressure heat capacity, C_p, as a function of temperature, the transition temperature was obtained at a given pressure. However, the most difficult problem encountered in the construction of this diagram was the problem of quasiergodicity. That problem was due to the improper exploration of the PES and caused large uncertainties in the average value of properties that were measurements of the fluctuation of mechanical variables. An example of this is the computation of C_p in the *NPT* ensemble, which measures the fluctuation in the enthalpy of the system. To circumvent the problem, Ortiz *et al.* [10] presented an extension of the *J*-walking formalism to the isothermal-isobaric ensemble. Specifically, the standard random walker at a desired temperature and pressure is coupled with a walker at a

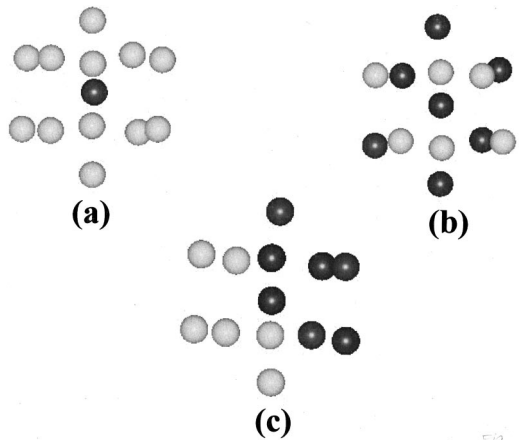

FIG. 1. Three possible spatial arrangements for a 13-atom alloy cluster: (a) cherry model, (b) completely mixed, and (c) completely segregated system.

*Author to whom correspondence should be addressed. Email address: g_lopez@rumac.upr.clu.edu

different temperature and pressure which samples configurational/volume space more efficiently. Jumps are attempted to this walker periodically with a non-Boltzmann sampling distribution that satisfies detailed balance. The method was successfully applied to the study of the solid-liquid equilibrium for Ar_{55}.

In the present work, the *J*-walking Monte Carlo method in the isothermal-isobaric ensemble is applied in the characterization of the order-disorder phase transition of Ni_7Pd_6. This method has been used because previous studies [3,11,12] on alloy clusters have shown that the standard Metropolis technique fails to predict order-disorder transitions at low temperature. This study will provide a clear and complete thermodynamic description of this transition. Moreover, unlike previous studies [3,11,12], the effect of pressure on this transition is considered. By defining a spherical volume, the variation in the low-temperature transition is considered as a function of pressure and a fixed composition.

In Sec. II of this paper the theoretical methods used are described. In Sec. III, the results are presented and discussed. Finally, in Sec. IV, we summarize our findings and suggest directions for future work.

II. THEORETICAL MODELS

A. Interparticle potential

It is well known that simple pairwise potentials do not provide an accurate description of the interparticle interaction in metallic systems. In particular, many-body effects play a crucial role in the proper description of these systems. However, previous studies [3,14] have shown that when many-body empirical potentials are applied to the study of structural changes as a function of temperature, no significant differences are observed when compared with the simple pairwise potential. Hence, as in our previous studies [3,5,7,10], Lennard-Jones potentials have been used to model the interaction between atoms. In the Lennard-Jones potential, the interaction between any pair of atoms *i* and *j* is given by

$$V(r_{ij}) = 4\varepsilon_{ij}\left[\left(\frac{\sigma_{ij}}{r_{ij}}\right)^{12} - \left(\frac{\sigma_{ij}}{r_{ij}}\right)^{6}\right], \tag{1}$$

where r_{ij} is the distance between atoms *i* and *j*, and ε_{ij} and σ_{ij} define the energy and the length units, respectively. For the bimetallic system considered here, $\varepsilon_{\text{Ni-Ni}} = 6030\,\text{K}$, $\sigma_{\text{Ni-Ni}} = 2.282\,\text{Å}$, $\varepsilon_{\text{Pd-Pd}} = 4951\,\text{K}$, and $\sigma_{\text{Pd-Pd}} = 2.520\,\text{Å}$. To calculate the interaction between unlike species, the Berthelot-Lorentz combining rules [2] have been used:

$$\varepsilon_{ij} = \frac{\sigma_{ii} + \sigma_{jj}}{2}, \tag{2}$$

$$\varepsilon_{ij} = \sqrt{\varepsilon_{ii}\varepsilon_{jj}}. \tag{3}$$

To define the cluster, a constraining potential [15] has been used and is defined as a perfectly reflecting wall centered at the center of mass of the cluster, which has a constraining radius R_c. For all calculations in this work, the constraining radius is set at 3 Å.

B. Isothermal-isobaric ensemble and *J*-walking Monte Carlo

In the standard Metropolis Monte Carlo algorithm [16], a random walker samples configuration space from an initial configuration r_i to a final configuration r_f with a probability of acceptance, *p*, which is given by [17]

$$p = \min[1, q(r_f, r_i)], \tag{4}$$

where $q(r_f, r_i)$ is given by

$$q(r_f, r_i) = \frac{S(r_i|r_f)\rho(r_f)}{S(r_f|r_i)\rho(r_i)}. \tag{5}$$

In this equation, $S(r_a|r_b)$ is the sampling distribution generated from a uniform deviate and $\rho(r)$ is the distribution function, which in the *NPT* ensemble is given by [18]

$$\rho(r) = \frac{\exp[-\beta(U+PV)]}{\Delta(N,T,P)}. \tag{6}$$

Here, U is the configurational energy, β is $1/k_BT$, P is the pressure, V is the volume, and $\Delta(N,P,T)$ is the isothermal-isobaric partition function. Hence, for this particular sampling distribution and distribution function,

$$q(r_f, r_i) = \exp[-\beta(\Delta U - P\Delta V)], \tag{7}$$

where ΔU and ΔV are the difference in configurational energy and volume between the final and initial states, respectively.

For the *J*-walking algorithm in the *NPT* ensemble [10], the sampling distribution is taken as a distribution at a temperature β_J and a pressure P_J,

$$S(r_f, r_i) = \frac{\exp\{-\beta_J[U(r_f) - P_J V(r_f)]\}}{\Delta(N,P,T)}. \tag{8}$$

To satisfy detailed balance, Eq. (5) is substituted into Eq. (2) to obtain

$$q(r_f, r_i) = \exp[(\beta_J - \beta)\Delta U + (\beta_J P_J - \beta P)\Delta V]. \tag{9}$$

As in the canonical ensemble, the *J*-walking method ensures detailed balance by jumping to a walker at a temperature and/or pressure that does not suffer from quasiergodicity problems Details of the implementation are presented in the next section.

C. Thermodynamic properties

Various thermodynamic properties are computed in the isothermal-isobaric ensemble. As usual, standard mechanical properties such as configurational energy and volume are computed as a function of temperature and pressure. Standard fluctuation expressions [19] are used for the characterization of the phase transitions. Namely, the variation in the constant pressure heat capacity, C_p, and the thermal compressibility, β_T, is computed as a function of temperature

and at a fixed pressure. The average value of C_p in the isothermal-isobaric ensemble is given by

$$\langle C_p \rangle = \frac{1}{k_B T^2} [\langle (U+PV)^2 \rangle - \langle (U+PV) \rangle^2] \qquad (10)$$

and the average value of β_T is given by

$$\langle \beta_T \rangle = \left\langle \frac{1}{k_B T \langle V \rangle} \right\rangle [\langle V^2 \rangle - \langle V \rangle^2]. \qquad (11)$$

The averages in Eqs. (10) and (11) are calculated using the previously presented *J*-walking method.

In order to implement the above method, a definition for the volume of the system must be provided. As in previous studies [9,10], we have assumed that the volume of the cluster is spherical and is given by

$$V = \frac{4\pi R^3}{3}, \qquad (12)$$

where R is obtained by adding the distance from the center of mass of the clusters to the outermost atom and the radius of the atom.

D. Characterization of atomic spatial arrangement

To characterize the arrangement of atoms in a specific cluster, the mixing number, M_N, is defined [2,3,20] as the number of unlike species bonds in that particular cluster. The mixing number provides a measurement of the heterogeneity in the cluster. For example, in the bimetallic icosahedral cluster, there are a total of 42 bonds; if the structure is completely segregated, the M_N value is 16, whereas, for a completely segregated cluster, the M_N value is 26.

Another useful tool for analyzing the nature of the spatial arrangement of the alloy clusters is the mixing number distribution function. The distribution of mixing number $[F(M_N)]$ measures the region of configurational space accessed by the *J*-walker for a cluster at a given mixing number. Moreover, $F(M_N)$ provides information about isomers sampled at a given temperature.

E. Computational details

The *J*-walking Monte Carlo method has been implemented in the following manner. A very long run consisting of 1×10^7 warm-up moves and 3×10^7 moves where data are gathered is used to generate the initial *J*-walking configuration. The pressure is fixed to 0 atm and the temperature to 3280 K. Under these thermodynamic conditions, where the cluster is in a gaslike form, configurations are saved in external arrays every 1000 steps. This distribution is used to generate additional *J*-walking distributions over a temperature range at a fixed pressure. Each additional *J*-walking distribution is generated when the acceptance ratio of jumps is less than 30%. To generate other curves at higher pressures, no additional distributions are needed because this same initial distribution is used, i.e., for $P>0$ atm, the value of $P_J = 0$ atm. On each external array, the configuration, volume, and configurational energy are stored. At temperatures where the *J*-walking configurations are not generated, the simulations are broken into 100 blocks with uncertainties calculated to one standard deviation. Each block consists of 10^5 warm-up moves and 10^5 moves where data are gathered. The starting configuration is the lowest-energy icosahedral structure that defines an initial volume of approximately 2135 Å^3.

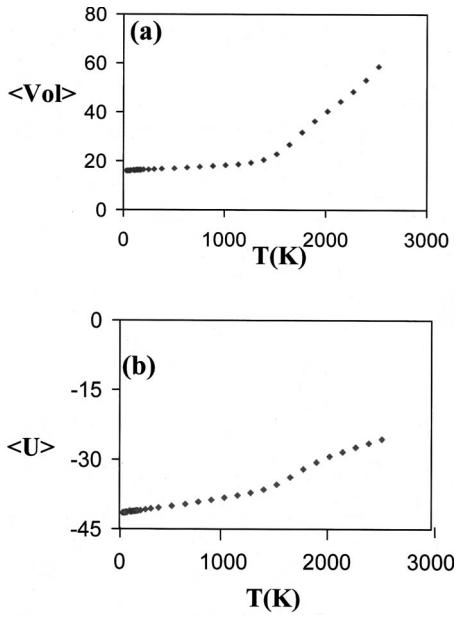

FIG. 2. Variation in (a) average volume and (b) configurational energy as a function of temperature at $P=0$ atm for Ni_6Pd_7.

III. RESULTS

Figure 2 shows the variation in volume and configurational energy as a function of temperature at $P=0$ atm. In both cases, at temperatures below 1500 K, small variations in these thermodynamic quantities are observed. For $T>1500$ K, an approximately linear increment in volume and energy is observed due to the coexistence of solidlike and liquidlike species, i.e., during the cluster-melting transition. The same behavior is observed in Fig. 3(a), where the isothermal compressibility, β_T, is presented as a function of temperature. At very low temperatures, the magnitude of β_T is very small, which is typical of solidlike materials. In the melting transition region, an increment in compressibility is observed due to the liquidlike form of the cluster. When the variation in $\langle C_p \rangle$ with temperature is analyzed [Fig. 3(b)], two transition regions can be identified. At high temperatures, the transition associated with cluster melting can be identified by a maximum temperature at $T_{\text{melting}}=1800$ K. However, at lower temperatures, a transition with a maximum at $T_{\text{mixing}}=136$ K (called here mixing temperature) is observed and, as previous studies in the canonical ensemble have shown [3,11,12], is associated with an order-disorder transition. When the behavior of $\langle \beta_T \rangle$ and $\langle V \rangle$ are analyzed in this low-temperature phase-transition regime, no significant variation is observed. This implies that the fluctuation in the enthalpy of the system, which causes the anomalies in C_p, is basically due to the fluctuation in configurational en-

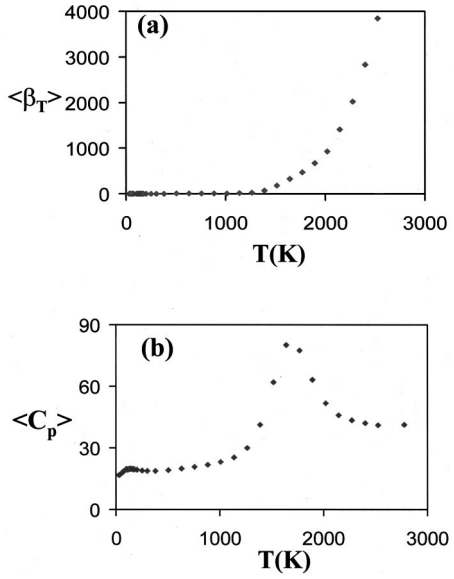

FIG. 3. Variation in (a) isothermal compressibility and (b) constant pressure heat capacity as a function of temperature at $P=0$ atm for Ni_6Pd_7.

ergy as the cluster jumps between segregated and mixed structures.

Figure 4 shows the distribution of the mixing number, $F(M_n)$, as a function of the mixing number at three temperatures and $P=0$ atm. At temperatures below $T_{\text{mixing}}=136$ K, the random walker only explores configurations with a segregated structure that has a value of $M_n=16$. As the temperature increases, structures with higher mixing number are sampled and at $T_{\text{mixing}}=136$ K a coexistence of clusters with $M_n=16$, 18, 20, 22, and 24 can be identified. The coexistence of isomers with different spatial arrangements is what has been called [3,11,12] the order-disorder transition. Figure 4 also shows the values of $F(M_n)$ as a function of M_n at $T=176$ K and no significant change is observed when compared to the distribution at T_{mixing}.

Figure 5 shows the variation in the constant-pressure heat capacity as a function of temperature at different values of pressures. It can be observed that the value of T_{melting} slightly increases as the pressure increases. This result is similar to

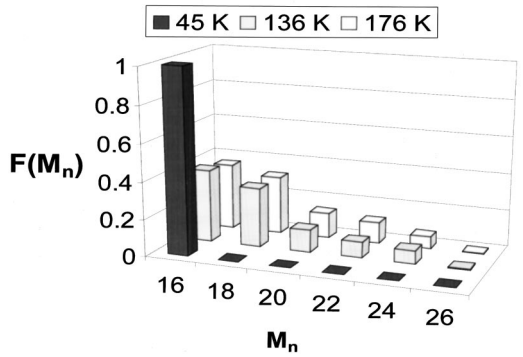

FIG. 4. Distribution of mixing number, $F(M_n)$, as a function of mixing number for Ni_6Pd_7 at three temperatures (45, 136, and 176 K) and $P=0$ atm.

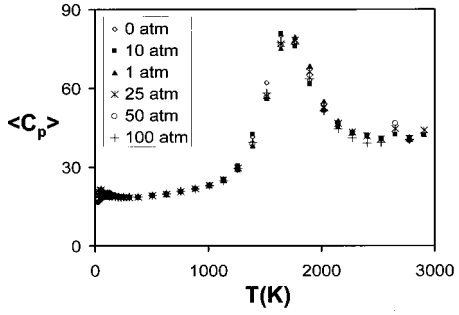

FIG. 5. Variation in the average constant pressure heat capacity, $\langle C_p\rangle$, as a function of temperature at six different pressures for Ni_6Pd_7.

previous computer simulations of the solid-liquid equilibrium for one-component clusters [9,10]. In the case of the order-disorder transition, a quite different behavior is observed. Figure 6 shows the variation in $\langle C_p\rangle$ as a function of temperature at various pressures but in the low-temperature regime. It can be seen that for $P<25$ atm, as the pressure is increased, the value of T_{mixing} is shifted towards lower temperatures and, hence, becomes smaller. A possible explanation for this phenomenon, based on thermodynamic arguments, is the following. The Gibbs free energy for any isolated system varies with temperature in the form shown in Fig. 7. This variation is established by the fundamental thermodynamic equation

$$dG=-SdT+VdP \tag{13}$$

and its Maxwell forms

$$\left(\frac{\partial G}{\partial T}\right)_P=-S, \quad \left(\frac{\partial G}{\partial P}\right)_T=V. \tag{14}$$

For a solid phase S_1, a negative slope for the G-T plot is observed due to the increment in entropy as the temperature increases. A second solid phase, S_2, is also depicted in Fig. 7 with a steeper slope because the entropy of this phase is larger. In our case, S_1 and S_2 correspond to the segregated and mixed phases, respectively. The point where the two curves intersect, $G_1=G_2$, defines the transition temperature (in this study T_{mixing}). The increase in the value of G with pressure at a given temperature is given by the volume of the

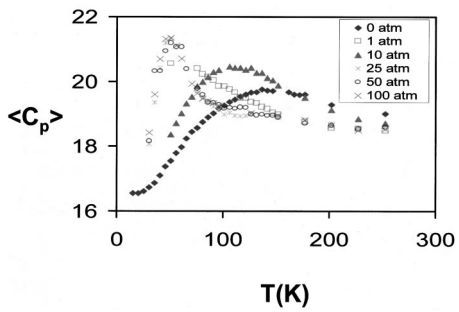

FIG. 6. Variation in the average constant pressure heat capacity, $\langle C_p\rangle$, as a function of temperature at six different pressures in a low-temperature regime for Ni_6Pd_7.

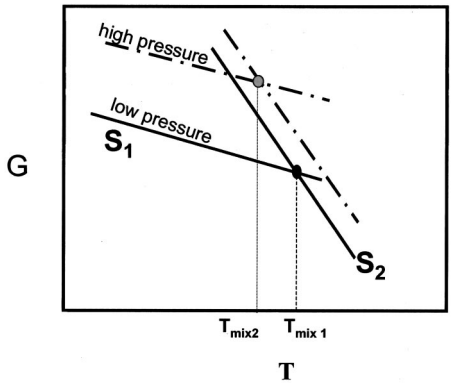

FIG. 7. Sketch of the variation in the Gibbs free energy (G) with temperature for an isolated system. The lines show schematically the effect of increasing pressure on the Gibbs free energy.

phase. From Fig. 8 it can be seen that the volume of phase S_1 is larger than the volume of S_2 at all temperatures and the two pressures presented. Therefore, the increase in the G-T curves for S_1 is larger than the increase in the S_2 curve and the intersecting of the two curves occurs at a lower temperature. Hence, a decrease in T_{mixing} is expected as the pressure of the system increases.

Another important feature shown in Fig. 6 is that as the pressure is increased, the width of the peak becomes smaller. Also, for pressure larger than 25 atm, the shape and the location of the peak do not vary much. In order to fully understand the behavior of this order-disorder transition, the distribution of mixing numbers is computed at various

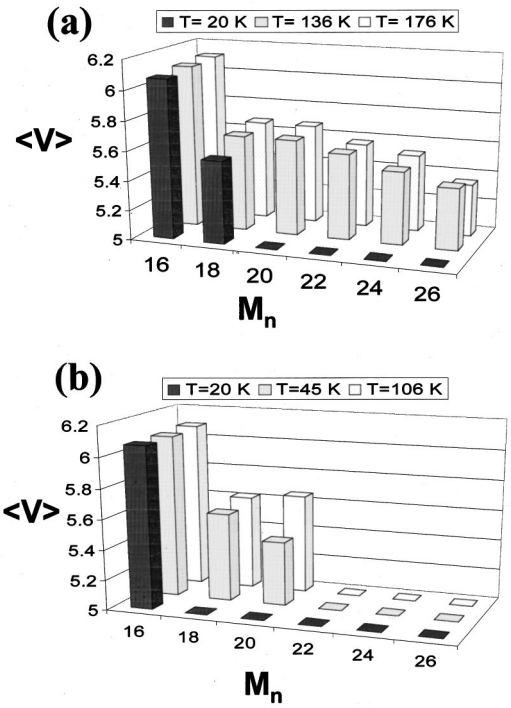

FIG. 8. (a) Average volume for different mixing numbers at three different temperatures (45, 136, and 176 K) and $P=0$ atm. (b) Same as (a) but at 20, 45, and 106 K for $P=25$ atm.

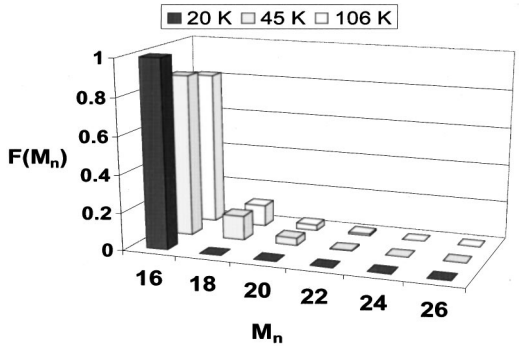

FIG. 9. Distribution of mixing number, $F(M_n)$, as a function of mixing number for Ni_6Pd_7 at three temperatures (45, 136, and 176 K) and $P=25$ atm.

temperatures and at a pressure different from zero. Figure 9 shows this distribution for $P=25$ atm. It can be seen that at very low temperatures only the $M_n=16$ isomer is sampled, similar to what was discussed for $P=0$ atm. However, at $T=45$ K (T_{mixing} at this pressure), isomers with $M_n=16$, 18, and 20, which are responsible for the anomaly in the heat capacity, are explored. At $T>T_{\text{mixing}}$, no significant change is observed in the distribution of mixing numbers. The above arguments, associated with the isomeric sampling as a function of pressure, are the reasons for the broadening of the transition peak as the pressure is decreased. Namely, because a larger number of isomers with different mixing numbers are sampled at $P=0$ atm, the peak becomes wider when compared to the distribution at $P=25$ atm.

IV. CONCLUSIONS

In the present study, the order-disorder and melting phase transition for a Lennard-Jones bimetallic cluster have been considered using the newly developed isothermal-isobaric ensemble J-walking Monte Carlo method. The behavior of the melting transition is similar to what is observed for one-component clusters, namely, as the pressure is increased, small increments in the value of T_{melting} are observed. On the other hand, a low-temperature transition is observed and is associated with an order-disorder transition. The variation of this transition with pressure is very different from what is observed for the melting transition. In a low-pressure range ($0<P<25$ atm), the mixing temperature decreases as the pressure of the system increases. However, for values of $P>25$ atm, no variation in the mixing temperature is observed. Computation of the mixing number as a function of temperature and pressure clearly explains the nature of the order-disorder transition. Also, simple thermodynamic arguments are used to validate the obtained results.

As stated previously, simple pairwise interparticle potentials were used to model this metallic system. The nature of these interactions for real physical systems is far more complex than the ones used here. However, it can be expected that various real bimetalli cluster systems exhibit this low-temperature phase transition.

Previous studies [11,12] have shown that the physical behavior of 13-atom LJ alloy clusters is independent of the

composition of the cluster. Only small variations in the magnitude of the constant volume heat capacity at the transition temperature are observed. At present, the variation in the low-temperature phase transition as a function of composition and pressure is being considered using the newly developed method presented here. Such a study will provide information for the construction of phase diagrams for binary systems. Also, larger clusters, where significant variations in composition can have an important effect, are under study. The effect of cluster size will also be considered and compared with previous results [9,21] for pure systems. It will be expected that as the size of the cluster increases, the transition temperatures will tend to the values of the same system in bulk. Quantum effects are being incorporated using a newly developed isothermal-isobaric ensemble.

ACKNOWLEDGMENTS

The NSF-EPSCoR program supported this work. G.E.L. is supported by the Henry and Camille Dreyfus Foundation.

[1] R. D. Gonzalez, Appl. Surf. Sci. **19**, 18 (1984).
[2] M. Nieves, I. M. Quintana, and G. E. López, Microchemical J. **55**, 254 (1997).
[3] G. E. López and D. L. Freeman, J. Chem. Phys. **98**, 1428 (1993).
[4] R. H. Berry, T. L. Beck, and H. L. Davis, *Advances in Chemical Physics* (Wiley, New York, 1988).
[5] N. Y. Matos and G. E. López, J. Chem. Phys. **109**, 1141 (1998).
[6] D. D. Frantz, D. L. Freeman, and J. D. Doll, J. Chem. Phys. **93**, 2769 (1990).
[7] G. E. López, J. Chem. Phys. **104**, 6650 (1996).
[8] A. J. Acevedo, L. Caballero, and G. E. López, J. Chem. Phys. **106**, 7257 (1997).
[9] H. P. Cheng, X. Li, R. L. Whetten, and R. S. Berry, Phys. Rev. A **46**, 791 (1992).
[10] W. Ortiz, A. Perlloni, and G. E. López, Chem. Phys. Lett. **298**, 66 (1998).
[11] D. D. Frantz, J. Chem. Phys. **105**, 10 030 (1996).
[12] D. D. Frantz, J. Chem. Phys. **107**, 1992 (1997).
[13] C. Kittle, *Introduction to Solid State Physics*, 4th ed. (Wiley, New York, 1971).
[14] D. G. Vlachos, L. D. Schmidt, and R. Aris, J. Chem. Phys. **96**, 6891 (1992).
[15] J. K. Lee, J. A. Barker, and F. F. Abraham, J. Chem. Phys. **58**, 3166 (1973).
[16] N. Metropolis, A. Rosenbluth, M. N. Rosenbluth, A. Teller, and E. J. Teller, J. Chem. Phys. **21**, 1087 (1953).
[17] M. H. Kalos and P. A. Whitlock, *Monte Carlo Methods* (Wiley, New York, 1986).
[18] M. P. Allen and J. Tildesley, *Computer Simulations of Liquids* (Oxford Science, Oxford, 1987).
[19] T. L. Hill, *An Introduction to Statistical Thermodynamics* (Dover, New York, 1986).
[20] M. Ocasio and G. E. López, J. Chem. Phys. **112**, 3339 (2000).
[21] P. Labastie and R. L. Whetten, Phys. Rev. Lett. **65**, 1567 (1990).